
Optical Properties of Langbeinites

II. Domain structure observation

R.Vlokh, O.V.Vlokh, I.Skab, I.Girnyk

Institute of Physical Optics, laboratory of gradient optics, polarimetry and phase transitions, 23 Dragomanov Str., 79005, Lviv, Ukraine, e-mail:vlokh@ifp.lviv.ua.

Received: 01.08.2002

Abstract

The review paper is devoted to the collection and analyze of experimental results obtained by different researches that have been investigating the domain structure in langbeinites by optical microscopy method. These investigations in general consist of studying the domain structure in ferroelectrical langbeinites $(\text{NH}_4)_2\text{Cd}_2(\text{SO}_4)_3$ and $\text{Rb}_2\text{Cd}_2(\text{SO}_4)_3$ and studying the “forbidden” domain walls in ferroelastical langbeinites - $\text{K}_2\text{Cd}_2(\text{SO}_4)_3$, $\text{K}_2\text{Mn}_2(\text{SO}_4)_3$ and solid solutions on their base as well as $\text{Tl}_2\text{Cd}_2(\text{SO}_4)_3$, $\text{K}_2\text{Co}_2(\text{SO}_4)_3$ ferroelastics. It was shown that “forbidden” domain walls should be considered as separate kind of thick (few tens of micrometers) walls that consist of the paraelastic phase layers. In a peculiar case of ferroelastic langbeinites these domain walls exist only due to the possibility of appearance high temperature phase (parent phase) with the point group of symmetry $43m$. The orientation of domain walls is discussed following from thermodynamic theory.

PACS: 42.33.SS-b.,77.80.B,78.20.Jq,78.30.-J

Keywords: langbeinites, domain structure, optical microscopy

Contents (Continuation)

Introduction

1. Electrooptical effect (in the previous issue)
2. Optical activity and circular dichroism spectrums (in the previous issue)
3. Domain structure observation (in the present issue)
4. Birefringence studying at phase transitions (in next issue)
5. Raman scattering spectrums (in next issue)

Conclusions

Introduction

The most interesting problem in langbeinites is the problem of phase transitions. The ferroelectricity in langbeinites was first found in $(\text{NH}_4)_2\text{Cd}_2(\text{SO}_4)_3$ crystals by E.Jona and R.Pepinsky in 1956 [1]. In general langbeinites possess two sequences of phase transitions: $\text{P}_{2_1}3\text{FP}_{2_1}2_1$ and $\text{P}_{2_1}3\text{FP}_{2_1}\text{FP}_{1\text{FP}_{2_1}2_1}$ [2]. The phases with a space group of symmetry P_{2_1} and P_1 are improper ferroelectric as the phase with symmetry $\text{P}_{2_1}2_1$ is proper ferroelastic [2,3]. The phase transition temperatures and change of the symmetry in different langbeinites

are presented in Table 1. It is interesting to note that according to the phenomenological theory proposed by V.Dvorak the existing improper ferroelectrical phase with a space group of symmetry R_3 was also predicted [2,3].

Some problems of the phase transitions in langbeinites have not been solved yet. For example on hydrostatic pressure in pure langbeinites [6-8] and in the solid solutions of langbeinites [9-11] new phases with unknown symmetry and nature appeared on the P,T – and x,T – phase diagrams. The “forbidden” [12] domain structure in ferroelastic phases of

Table 1. Phase transitions in langbeinites.

Classification	Scheme of the phase transition	Crystal	Abbreviated name	T ₃ , K	T ₂ , K	T ₁ , K
Group I	P2 ₁ 3	(NH ₄) ₂ Cd ₂ (SO ₄) ₃	(ACS)	-	-	95
	↓	(NH ₄) ₂ Mg ₂ (SO ₄) ₃	(AMgS)	-	-	221
	P2 ₁	(NH ₄) ₂ Ca ₂ (SO ₄) ₃	(ACaS)	-	-	158
	↓	(NH ₄) ₂ Ni ₂ (SO ₄) ₃	(ANS)	-	-	160
	P1	Tl ₂ Cd ₂ (SO ₄) ₃	(TCS)	92	120	128
	↓	Rb ₂ Cd ₂ (SO ₄) ₃	(RCS)	68	103	129
	P2 ₁ 2 ₁ 2 ₁	K ₂ Zn ₂ (SO ₄) ₃	(KZS)	75	-	138
Group II	P2 ₁ 3	K ₂ Mn ₂ (SO ₄) ₃	(KMS)	197	-	-
	↓	Rb ₂ Ca ₂ (SO ₄) ₃	(RCaS)	183	-	-
	P2 ₁ 2 ₁ 2 ₁	K ₂ Cd ₂ (SO ₄) ₃	(KCS)	432	-	-
		K ₂ Co ₂ (SO ₄) ₃	(KCoS)	126	-	-
		K ₂ Ca ₂ (SO ₄) ₃	(KCaS)	-	-	-
	not determined	K ₂ Fe ₂ (SO ₄) ₃	(KFS)	130	-	-
Group III	no transition	(NH ₄) ₂ Mn ₂ (SO ₄) ₃	(AMS)			
		Tl ₂ Mn ₂ (SO ₄) ₃	(TMS)			
		K ₂ Mg ₂ (SO ₄) ₃	(KMgS)			
		Rb ₂ Mg ₂ (SO ₄) ₃	(RMgS)			
		Cs ₂ Ca ₂ (SO ₄) ₃	(CsCaS)			
		Rb ₂ Mn ₂ (SO ₄) ₃	(RMS)			
		(NH ₄) ₂ Co ₂ (SO ₄) ₃	(ACoS)			
		Rb ₂ Co ₂ (SO ₄) ₃	(RCoS)			
		Tl ₂ Co ₂ (SO ₄) ₃	(TCoS)			
		(NH ₄) ₂ Ni ₂ (SO ₄) ₃	(ANS)			
		K ₂ Ni ₂ (SO ₄) ₃	(KNS)			
		Rb ₂ Ni ₂ (SO ₄) ₃	(RNS)			

langbeinites [13-18] also appeared before our study of the unsolved problem. It means that these crystals are still interesting from the point of view of phase transitions.

In the present part of the review we would like to present the results of investigations of the domain structure in langbeinite crystal family by optical methods.

3. Domain structure observation

The studying of the domain structure of langbeinite crystals was started in 1972 by B.Brezina and M.Glogarova [19] from the

investigation of the Tl₂Cd₂(SO₄)₃ crystals that possess a full sequence of phase transitions. The domains found which appeared in P2₁ ferroelectric phase had the shape of layers and narrow wedges with the domain boundaries along <100> and <010> - directions. There also appeared domains separated by curved diffuse walls with (110) orientation. In the ferroelectric phase P1 domain structure was more complicated. The domains were separated by sharp domain walls with traces oriented along <100> and <110> - directions. In the other parts of the sample the domains with different

extinction positions were observed. The domain structure in $P2_12_12_1$ phase consists of three domains that were separated by sharp domain walls with the traces oriented along $\langle 110 \rangle$ i $\langle 110 \rangle$ - directions.

In our study of the domain structure of $Tl_2Cd_2(SO_4)_3$ crystals [20] the crystal plates of the $\langle 111 \rangle$ orientation with a thickness 0.91 mm were used. The reason of choosing the $\langle 111 \rangle$ direction for the observation of domains is connected with the orientation of the optical indicatrix in the neighboring domains. In the case of the ferroelastic phase transition in the langbeinite crystals, due to the piezooptical effect induced by the spontaneous deformations, extinction positions in the neighbor domains are the same if the direction of the observation coincides with the principle crystallographic axis. When the direction of observation is parallel to the $\langle 111 \rangle$ direction, the extinction positions in different domains differs by 30° and the domain structure can be visible.

The ferroelastic domain structure appeared at $T_{c3}=98K$ at cooling and was saved down to the liquid nitrogen temperature without any changes (Figure 1,a). We have observed three pairs of domains S2-S3', S1-S2' and S1-S3' with domain wall orientation between them – (110), (101) and (011), respectively (Fig. 1,b). The mechanical strains on the domain walls as well as regions of paraelastic phase [14] were not visible. The overlapping of the different domains in the direction of light propagation was observed. These domains disappeared on T_{c3} at heating. In the ferroelectric-ferroelastic phases with the point group of symmetry $P2_1$ and $P1$ we observed 90° domains which disappeared in the cubic phase.

On Figure 2 is presented the domain structure that appeared in $K_2Co_2(SO_4)_3$ crystals in the ferroelastic phase with symmetry $P2_12_12_1$ [21]. According to the authors two orientation states were observed: the first domain – a bright region with an extinction position parallel to the

$\langle 100 \rangle$ direction and the second domain – a dark region always extinct under the crossed polarizers. The study of the optical activity dispersion shows that in this domain optical activity is greater than linear birefringence and the direction of observation coincides with the quasioptical axis. On the other side, as it will be shown later, the dark regions can be isotropic thick domain walls between two orientation states (bright regions). In the other sample a third orientation state appeared with the extinction position parallel to the $\langle 100 \rangle$ - direction. The orientation of the domain walls was parallel to the $\{110\}$ planes.

Potassium-manganese sulfate crystals also belong to the group of pure ferroelastic langbeinite with a change of the point group of symmetry at phase transition 23F222. The domain structure of these crystals was studied by T. Hikita et al [4]. It was found that domains appeared at T_c and did not change their configuration down to liquid nitrogen temperature. Most of the domain walls were parallel to the $\langle 110 \rangle$ directions. The extinction of the domains occurred almost along $\langle 100 \rangle$ direction, but sometimes differed about 30° from the $\langle 100 \rangle$. In a few cases, domain walls of higher indices were observed. When the sample was heated passing T_c it sometimes cracked along the domain walls.

In the $K_2Mn_2(SO_4)_3$ crystal at the cooling rate we observed [17, 22] the appearance of ferroelastic domains at the $T_c=197K$ that exist in the whole temperature region below T_c . The observed domains belong to two ferroelastic orientation states and were separated by thick walls with an average thickness of $50\mu m$. These domain-phase walls were parallel to the $(\bar{1}10)$ -plane and are deviated from the mutually perpendicular position by an angle $\sim 19^\circ$. The region of the domain walls was optically isotropic and belonged to the cubic paraelastic phase (Figure 3a). At the next cooling the third orientation state sometimes appeared but strong

internal strains lead to its displacement from the crystal (Figure 3b). In the heating rate the movement of the phase boundary was usually observed. The orientation of interface was parallel to the (100) or (010) planes and the crystal was cracked along this planes.

The same sequence of phases is observed in potassium-cadmium sulfate [23]. For the first time the domain structure in these crystals was found by us in [24,15] (Figure 4). This domain structure exists only in a narrow temperature range below $T_c=432K$ ($\Delta T=2K$). In the samples with a thickness less than 0.66 mm the domain structure never appeared (Figure 5) [16]. At $T=T_c-2K$ crystals usually become single domains, but at fast cooling in some regions of the sample the domain structure was saved down to room temperature. The orientation of the phase boundary was determined as (100) (Figure 5) [16]. After more detail investigations of the domain structure in $K_2Cd_2(SO_4)_3$ crystals [14] we found that domain walls are parallel to $\{110\}$ planes and are thick walls with an average thickness of 16~40 μm . Domain walls deviate from a mutually perpendicular position at an angle $\sim 10^\circ$. Moreover, the paraphase plays the role of the domain boundaries and this region is optically isotropic (Figure 6) [14].

All solid solutions $K_2Cd_{2x}Mn_{2(x-1)}(SO_4)_3$ that were obtained by the Czochralski and Bridgman method of growth [25] as well as pure $K_2Cd_2(SO_4)_3$ and $K_2Mn_2(SO_4)_3$ crystals possess only one ferroelastical phase transition with a change of the point group of symmetry 23F222 [26]. The x, T -phase diagram studied by us is shown on Figure 7. Only one point (isolated point) of the second order phase transition at $x=0.8$ on the line of first order phase transitions exists on this phase diagram. The domain structure of $K_2Cd_{1.6}Mn_{0.4}(SO_4)_3$ solid solution [18] that possesses a second order phase transition is presented on Figure 8. As it is visible the domain walls in these crystals are usual walls with orientation directly parallel to the (110)-plane without any deviation from the

mutually perpendicular positions. It is interesting to note also that the region of the paraphase does not play the role of a domain boundary in $K_2Cd_{1.6}Mn_{0.4}(SO_4)_3$ solid solution and that we did not find the region of paraphase between domains in $Tl_2Cd_2(SO_4)_3$ crystals because the phase with symmetry 222 in $Tl_2Cd_2(SO_4)_3$ is not in direct temperature contact with the cubic phase.

The description [14] of the existing and the orientation of the “forbidden” domain structure in the ferroelastic phase of langbeinites is based on the assumption of the existence of a parent phase in langbeinites (the conception of a parent phase with the symmetry $\bar{4}3m$ was proposed at first by D.Sannikov [27]). In such a case, in the phase with a symmetry 222, six domains can exist (three right and three left) and between some of enantiomorphic domains domain walls are permissible. At the second order phase transition the orientation of the domain walls should be directly $\{110\}$ as well as at the first order phase transition boundaries could deviate from mutually perpendicular orientation at some angle that is determined by the elastic compatibility of the domains.

The free energy describing the ferroelastic phase transition in ferroelastic langbeinites is given in the term of two independent strain components which construct the basis function of the two-dimensional irreducible representation of the point group 23 as follows [2]:

$$F = \alpha(u_1^2+u_2^2)+\delta_1u_1(u_1^2-3u_2^2)+\delta_2u_2(u_2^2-3u_1^2)+\beta(u_1^2+u_2^2)^2, \quad (1)$$

$$u_1=1/(6)^{1/2}(2e_{zz}-e_{xx}-e_{yy}), \quad (2)$$

$$u_2=1/(2)^{1/2}(e_{xx}-e_{yy}) \quad (3)$$

The rewritten eq.(1) in the polar coordinate (ρ, θ) is:

$$F = \alpha\rho^2+\delta_1\rho^3\cos 3\theta+\delta_2\rho^3\sin 3\theta+\beta\rho^4. \quad (4)$$

The stable configuration of θ - value is given by minimizing eq.(4) as

$$\theta_0=\pm 1/3\arctan\delta_2/\delta_1 \quad (5)$$

where the double sign corresponds to the

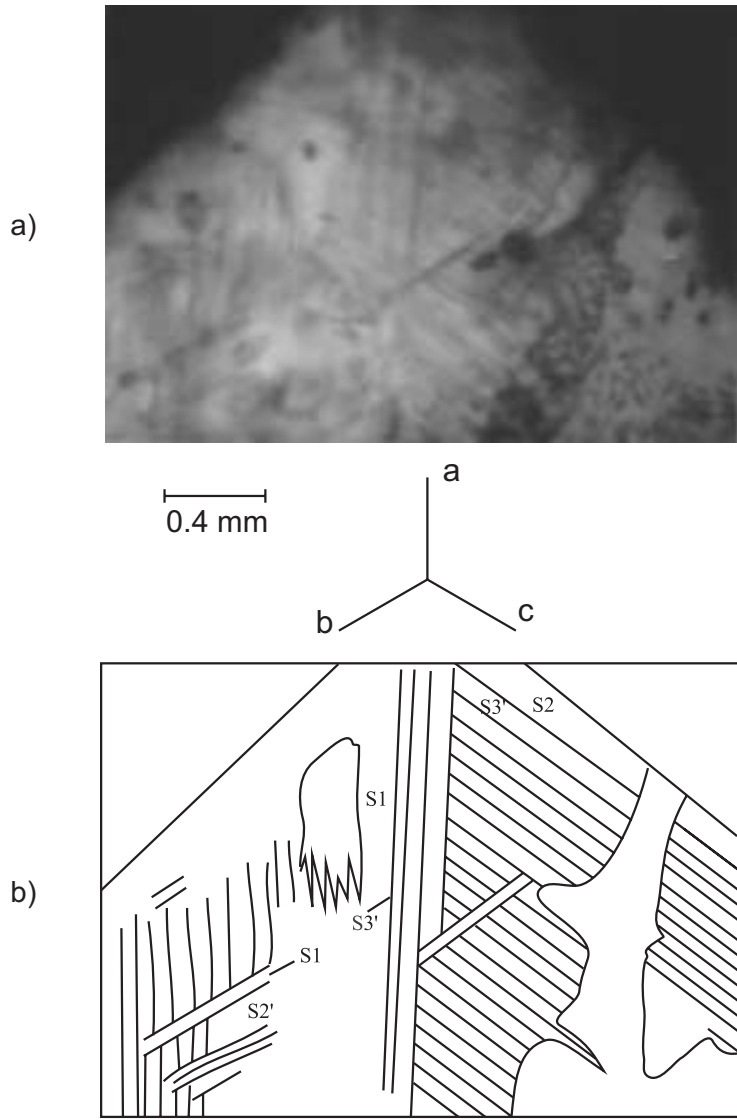


Figure 1. Ferroelastic domain structure in the TCS crystals ($T=91\text{K}$) (a) and schematic view of the three pairs of orientation states (b), schematic view (111-plate) [20].

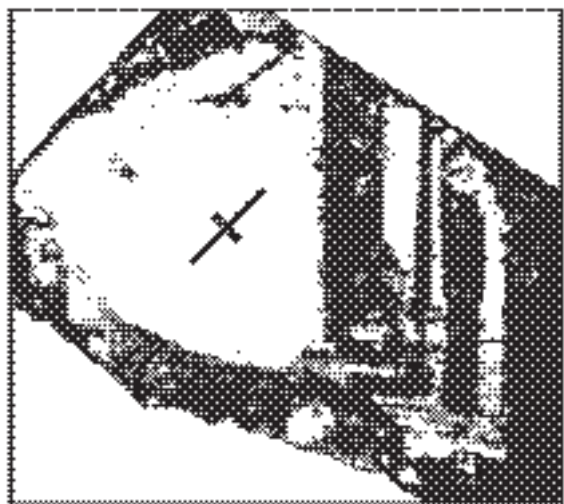


Figure 2. Domain structure of $\text{K}_2\text{Co}_2(\text{SO}_4)_3$ 21.

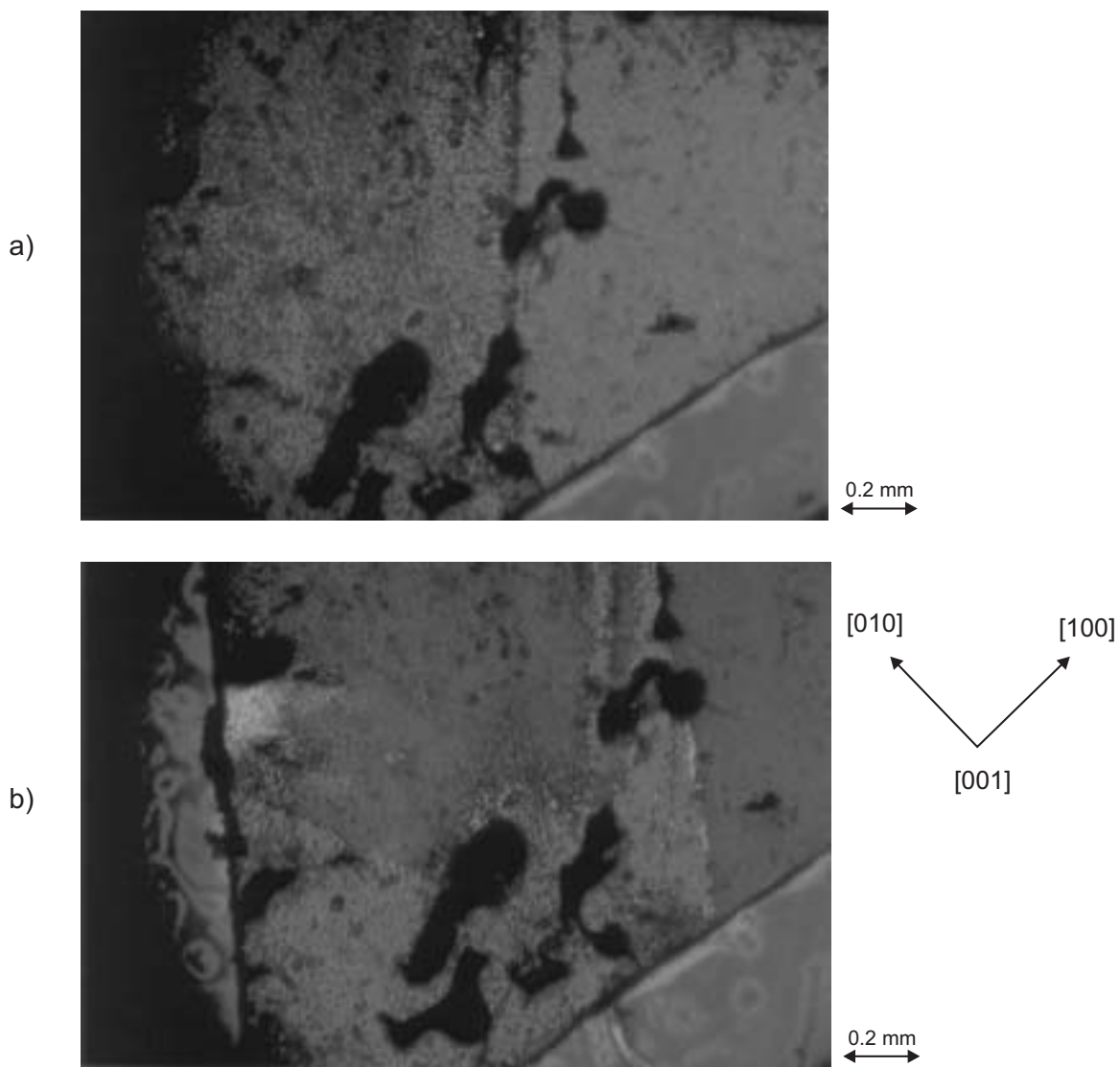


Figure 3. Domain structure of $K_2Mn_2(SO_4)_3$ crystals at the $T_c = 197K$: a) two orientation states; b) appearance of third orientation state (yellow region, violet region is the cubic phase) [17]

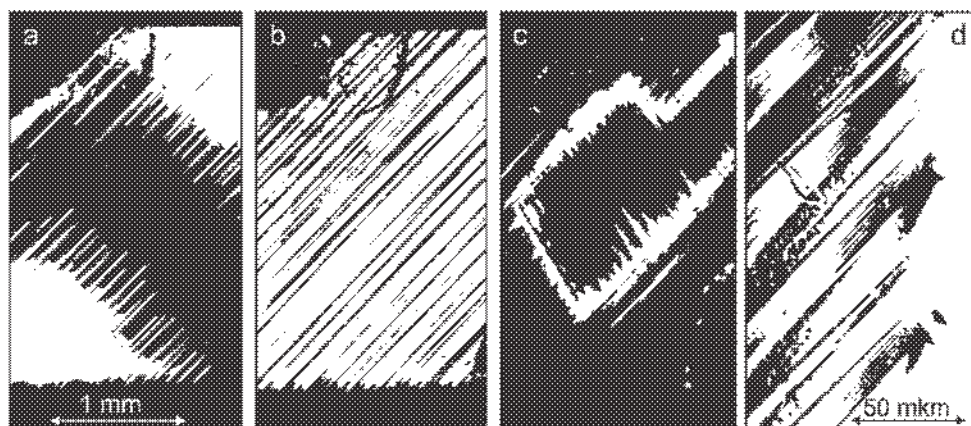


Figure 4. Domain structure of $K_2Cd_2(SO_4)_3$
 à) domain structure at $T_c = 432K$ (dark region - cubic phase);
 b) domain structure at $T = T_c - 0.4^\circ C$;
 c) domain blocks with different orientation of walls;
 d) complicate domain structure at room temperature.

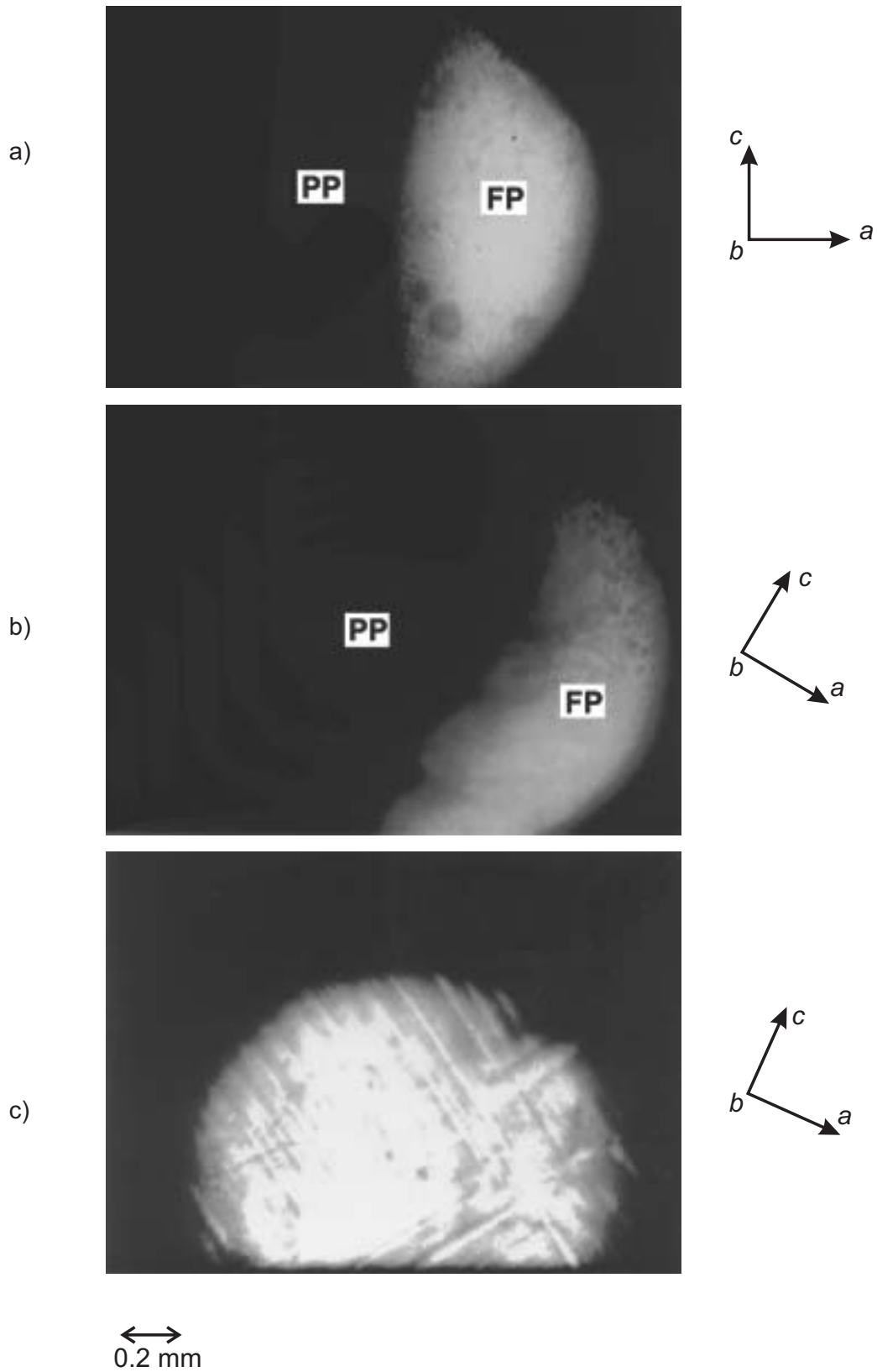
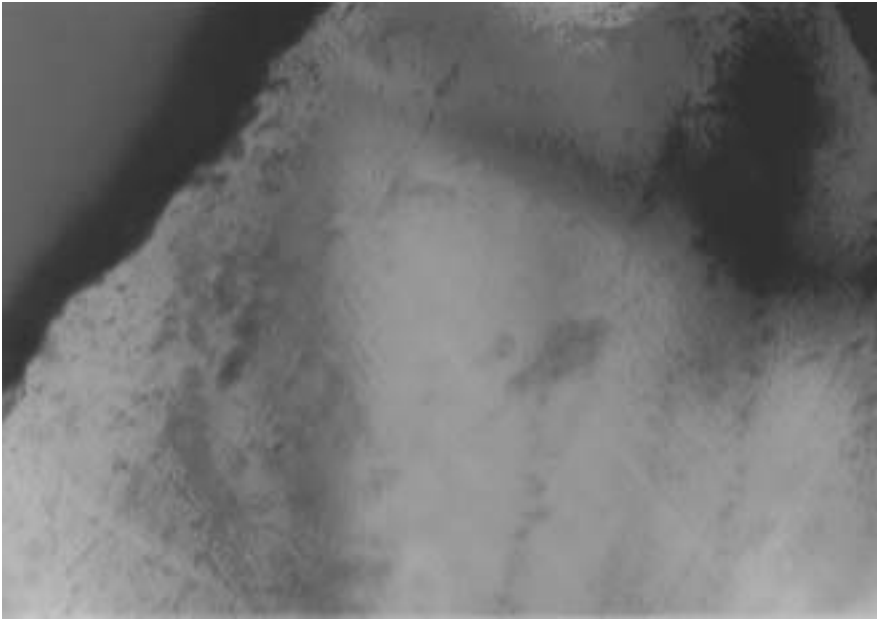


Figure 5. The phase boundary and the domain structure in $K_2Cd_2(SO_4)_3$: a) $d_b=0.26$ mm; b) $d_b=0.66$ mm (close phase boundary the domain structure is visible); c) $d_b=1$ mm [16].

<111> - plate

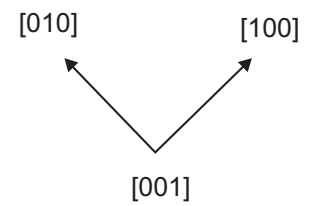
a)



0.1 mm

<001> - plate

b)



0.1 mm

Figure 6. Domain structure in $K_2Cd_2(SO_4)_3$: a) <111>plate; b) <001>plate; (violet region is the cubic phase)[14].

enantiomorphic modifications. In particular, when $\delta_1=0$, $\theta_o=\pm 30^\circ$ and the corresponding basis vector is identified to be u_2 . In such a case, the

$$\begin{aligned} \text{F1: } \varepsilon_1 &= \rho_o / (2)^{1/2} \begin{vmatrix} 1 & & \\ & -1 & \\ & & 0 \end{vmatrix} \\ \text{F2: } \varepsilon_2 &= \rho_o / (2)^{1/2} \begin{vmatrix} 0 & & \\ & 1 & \\ & & -1 \end{vmatrix} \\ \text{F3: } \varepsilon_3 &= \rho_o / (2)^{1/2} \begin{vmatrix} -1 & & \\ & 0 & \\ & & 1 \end{vmatrix} \end{aligned}$$

Here, the unprimed and primed domains are associated with different enantiomorphic modifications. In order to investigate the properties of the domain boundaries, we consider the difference of the spontaneous deformations between the domains originated from different enantiomorphic modifications. For instance, we have

$$\Delta\varepsilon(\text{S3}'-\text{S2}) = \varepsilon_3 - \varepsilon_2 = \rho_o / (2)^{1/2} \begin{vmatrix} -1 & & \\ & 1 & \\ & & 0 \end{vmatrix} \quad (7)$$

$$\Delta\varepsilon(\text{S1}-\text{S2}') = \varepsilon_1 - \varepsilon_2 = \rho_o / (2)^{1/2} \begin{vmatrix} -1 & & \\ & 0 & \\ & & 1 \end{vmatrix} \quad (8)$$

$$\Delta\varepsilon(\text{F1}-\text{F3}') = \varepsilon_1 - \varepsilon_3 = \rho_o / (2)^{1/2} \begin{vmatrix} 0 & & \\ & -1 & \\ & & 1 \end{vmatrix} \quad (9)$$

From the Sapriel theory, it is easily seen that well-defined $\{110\}$ - type domain boundaries should be formed between these domains.

The above described domain configuration corresponds to ferroelastic langbeinite crystals which are not far from the condition $\delta_1=0$ and the domain walls are planar with $\{110\}$ orientation. The absence of the mechanical strains on the domain walls and the regions of

spontaneous deformations for the six domains of the ferroelastic phase are simply given by the following strain tensor:

$$\begin{aligned} \text{F1': } \varepsilon_1 &= \rho_o / (2)^{1/2} \begin{vmatrix} -1 & & \\ & 1 & \\ & & 0 \end{vmatrix} \\ \text{F2': } \varepsilon_2 &= \rho_o / (2)^{1/2} \begin{vmatrix} 0 & & \\ & -1 & \\ & & 1 \end{vmatrix} \\ \text{F3': } \varepsilon_3 &= \rho_o / (2)^{1/2} \begin{vmatrix} 1 & & \\ & 0 & \\ & & -1 \end{vmatrix} \end{aligned} \quad (6)$$

the paraelastic phase between the domains means that the region of the elastic adaptation between the ferroelastic domains in TCS crystals is thin in comparison with KCS crystals and the values of the two diagonal components of the spontaneous deformation tensor are similar. Moreover, perhaps the paraelastic phase cannot appear as a domain wall in the case if the ferroelastic phase is not in the temperature contact with the paraelastic one. On the other hand the solid solutions that belong to the isolated point of second order phase transition on the phase diagram $\delta_1=\delta_2=0$ and as it was shown by us (Figure 8) the domain walls in $\text{K}_2\text{Cd}_{1.6}\text{Mn}_{0.4}(\text{SO}_4)_3$ are planar walls with orientation exactly parallel to the $\{110\}$ planes.

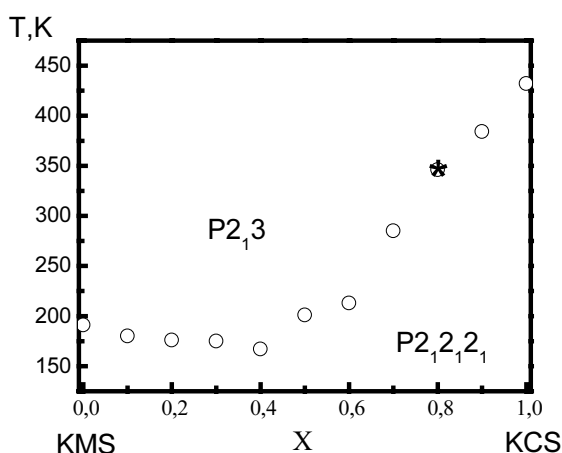


Figure 7. The x, T -phase diagram $\text{K}_2\text{Cd}_2\text{Mn}_{02(1-x)}(\text{SO}_4)_3$ solid solution [26].

The measuring of the topography of optical activity in the cubic 23 phase of $K_2Cd_{0.4}Mn_{1.6}(SO_4)_3$ solid solutions can be as the confirmation of the correctness of this approach. As it is visible from Figure 9 [18] the optical rotary power changes the sign in some parts of the sample. It means that phase enantiomorphic twins exist in the 23 and langbeinites possess the prototype phase with the point group of symmetry $\bar{4}3m$.

To determine domain walls orientation let us consider three cases:

- 1) domain walls between domains with different signs of enantiomorphism but with the same tensor of spontaneous deformation;
- 2) domain walls between domains with different signs of enantiomorphism and with different tensors of spontaneous deformation;
- 3) domain walls between domains with the same sign of enantiomorphism but with different tensors of spontaneous deformation:

1) planer permissible domain walls:

$$S1 - S1': \Delta\varepsilon (S1-S1') = \frac{2\rho_o}{\sqrt{2}} \begin{pmatrix} 1 & 0 & 0 \\ 0 & -1 & 0 \\ 0 & 0 & 0 \end{pmatrix} \Rightarrow$$

$$\Rightarrow \det\Delta\varepsilon=0 \Rightarrow x^2-y^2=0 \Rightarrow x=\pm y \Rightarrow (110) \& (1\bar{1}0)$$

$$S2 - S2': \Delta\varepsilon (S2-S2') = \frac{2\rho_o}{\sqrt{2}} \begin{pmatrix} 0 & 0 & 0 \\ 0 & 1 & 0 \\ 0 & 0 & -1 \end{pmatrix} \Rightarrow$$

$$\Rightarrow \det\Delta\varepsilon=0 \Rightarrow y^2-z^2=0 \Rightarrow y=\pm z \Rightarrow (011) \& (01\bar{1})$$

$$S3 - S3': \Delta\varepsilon (S3-S3') = \frac{2\rho_o}{\sqrt{2}} \begin{pmatrix} -1 & 0 & 0 \\ 0 & 0 & 0 \\ 0 & 0 & 1 \end{pmatrix} \Rightarrow$$

$$\Rightarrow \det\Delta\varepsilon=0 \Rightarrow z^2-x^2=0 \Rightarrow z=\pm x \Rightarrow (101) \& (\bar{1}01)$$

2) thick “quasipermissible” domain walls:

$$S1-S2': \Delta\varepsilon (S1-S2') = \frac{\rho_o}{\sqrt{2}} \begin{pmatrix} 1 & 0 & 0 \\ 0 & \cong 0 & 0 \\ 0 & 0 & -1 \end{pmatrix} \Rightarrow$$

$$\Rightarrow \det\Delta\varepsilon \approx 0 \Rightarrow x^2-z^2 \approx 0 \Rightarrow x \approx \pm z \Rightarrow (101) \& (10\bar{1})$$

$$S1 - S3': \Delta\varepsilon (S1-S3') = \frac{\rho_o}{\sqrt{2}} \begin{pmatrix} \cong 0 & 0 & 0 \\ 0 & -1 & 0 \\ 0 & 0 & 1 \end{pmatrix} \Rightarrow$$

$$\Rightarrow \det\Delta\varepsilon \approx 0 \Rightarrow z^2-y^2 \approx 0 \Rightarrow z \approx \pm y \Rightarrow (011) \& (0\bar{1}1)$$

$$S2 - S1': \Delta\varepsilon (S2-S1') = \frac{\rho_o}{\sqrt{2}} \begin{pmatrix} 1 & 0 & 0 \\ 0 & \cong 0 & 0 \\ 0 & 0 & -1 \end{pmatrix} \Rightarrow$$

$$\Rightarrow \det\Delta\varepsilon \approx 0 \Rightarrow x^2-z^2 \approx 0 \Rightarrow x \approx \pm z \Rightarrow (101) \& (10\bar{1})$$

$$S2 - S3': \Delta\varepsilon (S2-S3') = \frac{\rho_o}{\sqrt{2}} \begin{pmatrix} -1 & 0 & 0 \\ 0 & 1 & 0 \\ 0 & 0 & \cong 0 \end{pmatrix} \Rightarrow$$

$$\Rightarrow \det\Delta\varepsilon \approx 0 \Rightarrow y^2-x^2 \approx 0 \Rightarrow y \approx \pm x \Rightarrow (110) \& (\bar{1}10)$$

$$S3 - S1': \Delta\varepsilon (S3-S1') = \frac{\rho_o}{\sqrt{2}} \begin{pmatrix} \cong 0 & 0 & 0 \\ 0 & -1 & 0 \\ 0 & 0 & 1 \end{pmatrix} \Rightarrow$$

$$\Rightarrow \det\Delta\varepsilon \approx 0 \Rightarrow z^2-y^2 \approx 0 \Rightarrow z \approx \pm y \Rightarrow (011) \& (0\bar{1}1)$$

$$S3 - S2': \Delta\varepsilon (S3-S2') = \frac{\rho_o}{\sqrt{2}} \begin{pmatrix} -1 & 0 & 0 \\ 0 & 1 & 0 \\ 0 & 0 & \cong 0 \end{pmatrix} \Rightarrow$$

$$\Rightarrow \det\Delta\varepsilon \approx 0 \Rightarrow y^2-x^2 \approx 0 \Rightarrow y \approx \pm x \Rightarrow (110) \& (\bar{1}10)$$

3) between domains with the same sign of enantiomorphism domain walls are completely forbidden.

In the case of parent phase existing in langbeinites two kinds of domain walls in ferroelastic phase can exist:

- 1) planer permissible domain walls between enantiomorphic domains with the same orientation of spontaneous deformation tensor;
- 2) thick “quasipermissible” domain walls between enantiomorphic domains with different orientation of spontaneous deformation tensors.

It is obvious that walls of the second type can appear only at the satisfaction of the condition $\delta_1 \ll \delta_2$. The deviation of θ_0 from 30° leads to the appearing of transition zone with the well defined thickness between the domains.

The elastic modules [27a] and spontaneous deformations [27b] in $K_2Cd_2(SO_4)_3$ crystals increase with decreasing the temperature below T_c that leads to the rising of the energy of elastic adaptation. As $T \ll T_c$ single domain

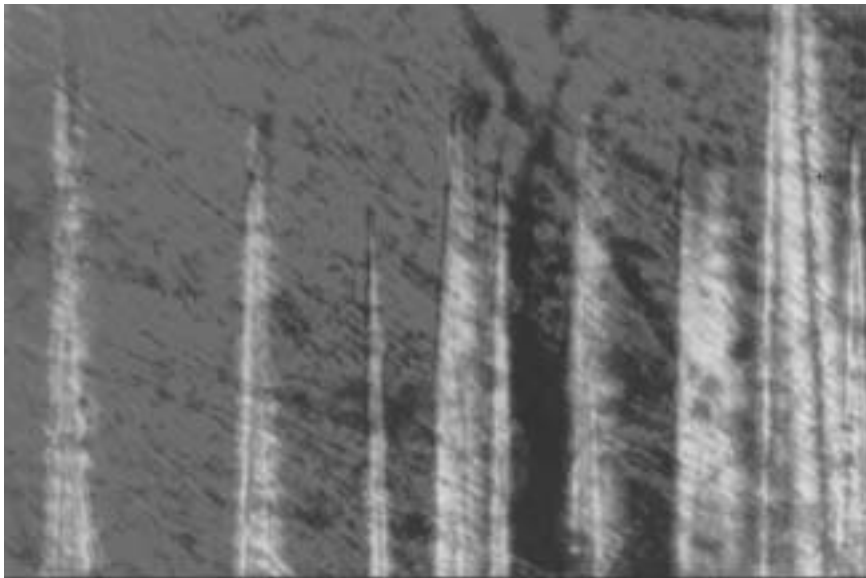


Figure 8. Domain structure of $K_2Cd_{1.6}Mn_{0.4}(SO_4)_3$ solid solution [18].

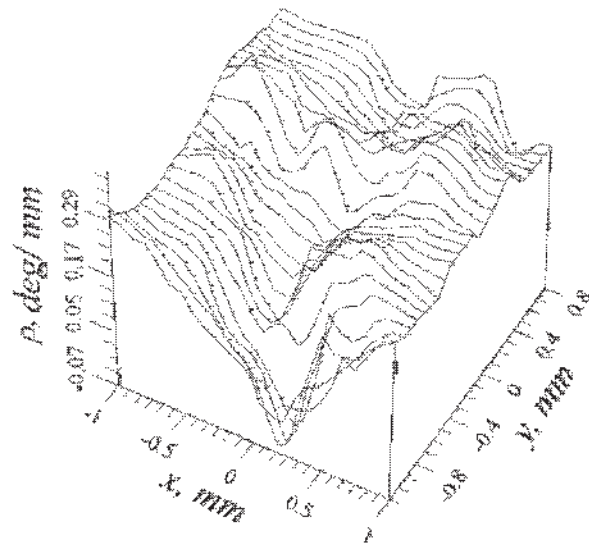


Figure 9. The topography of the optical activity in the 23 phase at room temperature of the $K_2Cd_{0.4}Mn_{1.6}(SO_4)_3$ crystals [18].

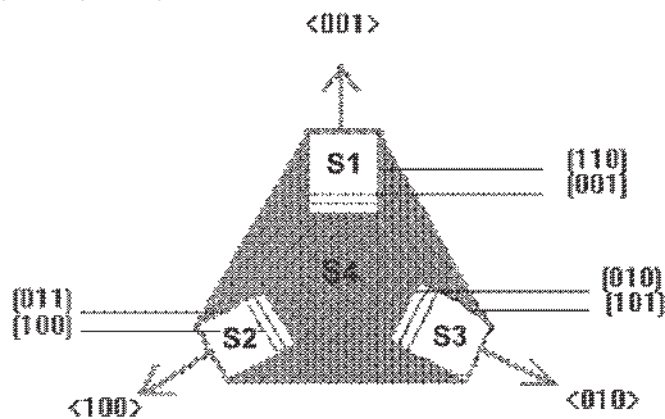
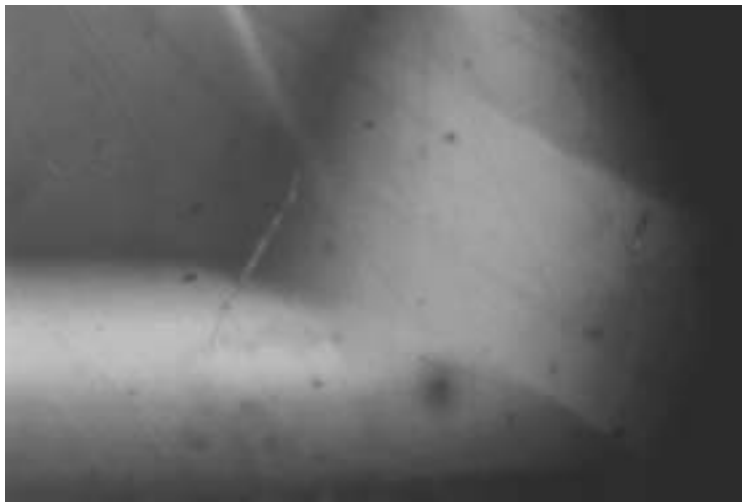
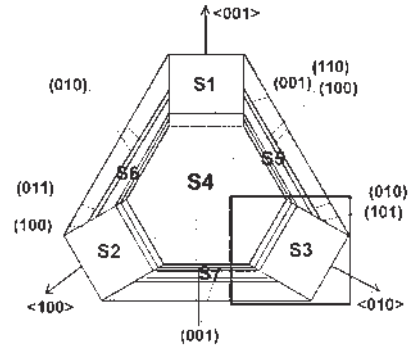


Figure 11. The domain structure in the $Rb_2Cd_2(SO_4)_3$ crystals at $T_1 < T < T_{c1}$ (schematic view, 111-plate). Four different domains exist in the sample - S1, S2, S3, S4.



0,2 mm

a)



b)

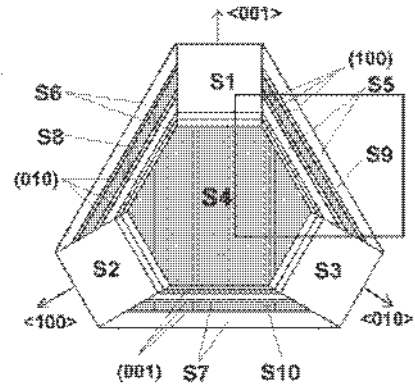
Figure 12. The domain structure in the $\text{Rb}_2\text{Cd}_2(\text{SO}_4)_3$ crystals at $T_{c2} < T < T_i$ (111-plate).

a) microfotograph b). schematic view [30].



0,2 mm

a)



b)

Figure 13. The domain structure in the $\text{Rb}_2\text{Cd}_2(\text{SO}_4)_3$ crystals at $T < T_{c2}$ (111-plate).

a) microfotograph; b) schematic view [30].

state becomes more preferable than multidomain ones and as the result the domain structure in potassium-cadmium langbeinite exists only in the range of few degrees below T_c . The $K_2Mn_2(SO_4)_3$ crystals possess weak temperature dependencies of spontaneous deformations and elastic modules [27c, 27d] and due to this - weak temperature dependence of the energy of elastic adaptation. It is the reason why the domain structure in $K_2Mn_2(SO_4)_3$ crystals exists at all temperature range below T_c .

On the base of temperature dependencies of lattice parameters of $K_2Cd_2(SO_4)_3$ and $K_2Mn_2(SO_4)_3$ crystals we calculated the phase of order parameter in the vicinity of T_c and it is equal 27.07° and 32.5° , respectively. It means that the angle θ depends on the concentration of x in $K_2Cd_{2x}Mn_{2(1-x)}(SO_4)_3$ solid solutions and the point with the magnitudes $\theta_G=3\theta^\circ$ i $\delta_l=0$ would exist on the x,T -phase diagram. These conditions correspond to the isolated point of the second order phase transition with ($x=0.8$). On the other side the condition $\delta_l=0$ is approximately satisfied for all solid solutions.

In the langbeinites that possess ferroelectric phase transitions domain structure was stu-

died in $Rb_2Cd_2(SO_4)_3$ [28] and $(NH_4)_2Cd_2(SO_4)_3$ [29] crystals. It is interesting to note that according to data [28] at $T=113K$ $Rb_2Cd_2(SO_4)_3$ crystals were singledomain (Figure 10).

The domain structure in the $Rb_2Cd_2(SO_4)_3$ crystals appeared at cooling process at $T=129K=T_{c1}$ [30]. As it is visible from Figure 11 at $T_1=113K<T<T_{c1}$ four different domains exist in the sample - S1, S2, S3, S4. The domain walls between central dark domains S4 and bright domains S1, S2 and S3: S1-S4, S2-S4 and S3-S4 are parallel to the (110), (011) and (101) planes, respectively. The domain walls between the central, dark part of the Figure 11 (domain S4) and the bright regions (domains S1, S2, S3) look like diffuse boundaries and are inclined to the surface of the crystal plate. These domain walls are parallel to the principle crystallographic planes (001), (100) and (010). So, one can conclude that in the $Rb_2Cd_2(SO_4)_3$ crystals in the temperature interval $T_1<T<T_{c1}$ simultaneously four different orientation states exist which are separated by three pairs of mutually perpendicular domain walls. The extinction positions in S1, S2 and S3 orientation states differ by 30° . It is interesting to note that domain S4 is extinct in any position between

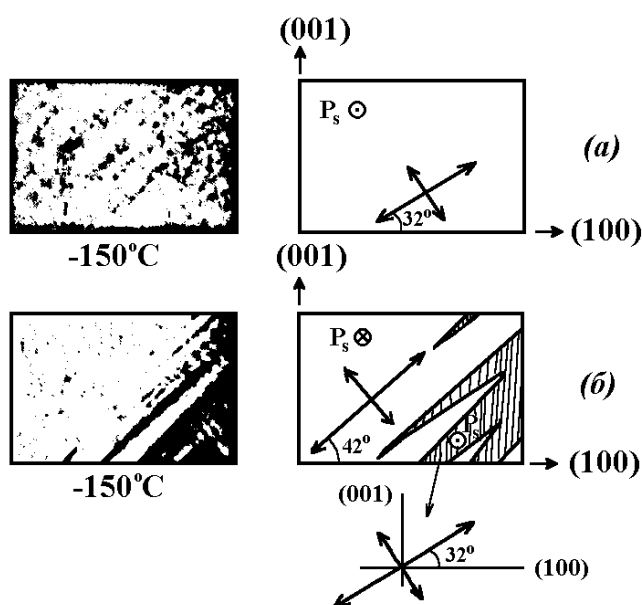


Figure 10. Photographs of domain patterns in (010) plate of annealed $Rb_2Cd_2(SO_4)_3$ crystal (a) poled upwards and (b) poled downwards under electric field of 50 kV/cm [28].

crosses polarizers. It means that the direction $\langle 111 \rangle$ in S4 domain in the temperature interval $T_i < T < T_{c1}$ coincides with the optically isotropy direction. At the temperature interval $T_{c2} = 103\text{K} < T < T_i$ the central and non-central dark parts of the sample become optically anisotropical (Figure 12). It means that below T_i new three domains S5, S6, S7 appeared in the $\text{Rb}_2\text{Cd}_2(\text{SO}_4)_3$ crystals. The domain walls between the central - hexagonal domain S4 and new S5, S6, S7 domains are inclined to the (111) surface and are parallel to the principle crystallographical planes. At T_i the movement of the phase boundary was not visible. The domain structure became more complicated (Figure 13). below T_{c2} The S5, S6 and S7 are splitted in to the layers like domains with domain walls parallel, perhaps, to the $\{100\}$ planes. At heating process we observed the changing of the domain structure in the back order.

The principle question on which we should find the answer after the above mentioned investigations is: if the T_i temperature is the temperature of phase transition or if it is the temperature of spontaneous polarization compensation due to the existance of the superlattice structure in the $\text{Rb}_2\text{Cd}_2(\text{SO}_4)_3$ crystals in the monoclinic phase? As it follows from data presented in [28] and [31] the spontaneous polarization and optical birefringence possess monotonic temperature dependence in the vicinity of T_i . It means that around T_i the domain structure should not be visible due to the absence of birefringence. But as it follows from the results of our observations - the domain structure exists at T_i and in the temperature range $T_i < T < T_{c1}$ four different orientation states exist. These domains possess different spontaneous deformations and one of them (S4) is optically single-axial. The optical axis of the S4 domain coincides with the $\langle 111 \rangle$ direction. It is necessary to note that at the ferroelectric-ferroelastic phase transition with the change of symmetry $23F3$ four orientation states could appear which differ in spontaneous

deformation tensor and the domain walls between them should be parallel to the $\{100\}$ and $\{110\}$ planes.

The paraelastic-paraelectric phase for the monoclinic phase with the point group of symmetry 2 in the langbeinite crystals is a cubic phase with the point group of symmetry 23. In this case according to the J.Sapriel theory [12] phase six orientation states and three types of domain walls with orientation (100), (010) and (001) could appear in the monoclinic. However, the domain walls with orientation $\{110\}$ are forbidden. The existance of domain walls which are parallel to the $\{110\}$ planes as well as the existance of seven orientation states in the monoclinic phase means - that the phases with the point group of symmetry 3 and 2 coexist at temperature below T_i . The domain walls with $\{110\}$ orientation which were observed in the monoclinic phase are the remain walls of the trigonal phase. As the confirmation of this fact is the presence of the broad maximum on the temperature dependence of dielectric permittivity around T_i (Figure 14).

On the basis of domain structure observation and temperature dependence of dielectric permittivity we can conclude that $T_i = T_{c4}$ is the temperature of diffuse phase transition between the trigonal and the monoclinic phase. As one can see (Figure 13) in the triclinic phase the view of the domain

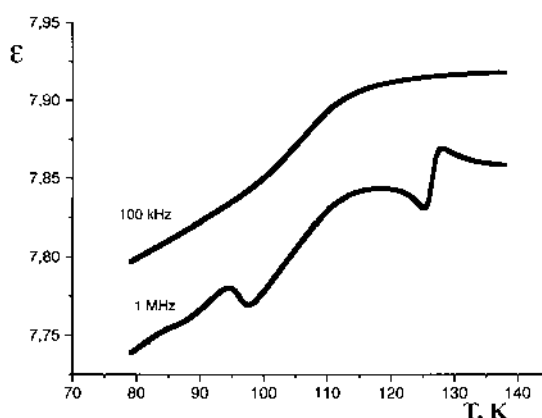


Figure 14. The temperature dependence of the dielectric permittivity of the $\text{Rb}_2\text{Cd}_2(\text{SO}_4)_3$ crystals measured in the $\langle 111 \rangle$ direction at 1 MHz and at 100 kHz [30].

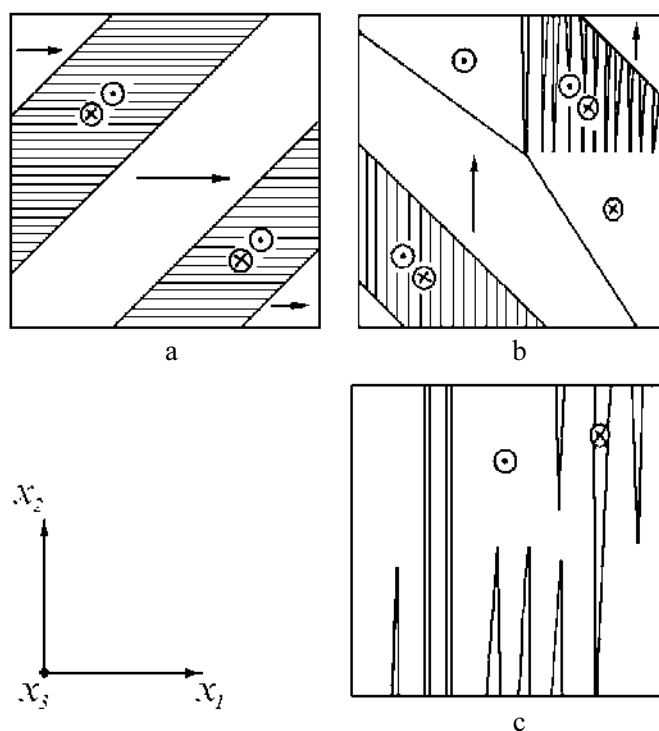


Figure 15. Domain structure of the $(\text{NH}_4)_2\text{Cd}_2(\text{SO}_4)_3$ crystals, (001)-plate) a) electrically isolated sample; b) electrically shorted sample; c) mechanically free sample [29].

structure is more complicated: inside S5, S6 and S7 domains new domains appeared and the domain walls which are separated these domains are inclined to the (111) - plane. In general, in this phase 12 orientation states could be observed and we found the increase of quantity of the domains at $T < T_{c2}$.

In the $(\text{NH}_4)_2\text{Cd}_2(\text{SO}_4)_3$ crystals that possess improper ferroelectrical phase transition with the change of symmetry 23F2 the domain structure which consists of the layers of domains with mutually perpendicular P_s -vectors, separated by (110)-walls (Figure 15,a) were observed [29]. At the same time the density system of the antiparallel domains with the difference in extinction on 18° was found. These domains were separated by permissible (010) or (100) walls. At the shorting of the (001)-sample of $(\text{NH}_4)_2\text{Cd}_2(\text{SO}_4)_3$ crystal, 180° -domains begin to occupy more place in the sample and the boundaries between 90° -domains possess orientation $\{570\}$ (Figure 15,b). The domain walls with (110) and $(1\bar{1}0)$ -orientations were also observed. These walls appeared due to the crossing of

the crystallographically nonequivalent domain walls (570) and (750) and are strained, non-permissible walls. The strains near the (110)-walls was compensated by the density net of the antiparallel domains. On the changing of the polarity of the applied electrical field 180° -domains were switched by the movement of the wedges with the permissible walls with (100) or (010) orientations (Figure 15,c).

(To be continued)

References

1. Jona E., Pepinsky R. Phys. Rev. **103** (1956) 1126.
2. Dvorak V. Phys. Stat. Sol. (b) **52** (1972) 93.
3. Dvorak V. Phys. Stat. Sol. (b) **66** (1974) K87.
4. Hikita T., Sato S., Sekiguchi H., Ikeda T. J. Phys. Soc. Jpn. **42** (1977) 1656.
5. Hikita T., Sekiguchi H., Ikeda T. J. Phys. Soc. Jpn. **43** (1977) 1327.
6. Hikita T., Kitabatake M., Ikeda T. J. Phys. Soc. Jpn. **49** (1980) 1421.
7. Glogarova M., Frenzel C., Hegenbarth E.

- Phys. Stat. Sol. (b) **53** (1972) 369.
8. Hikita T., Kitabatake M., Ikeda T. J. Phys. Soc. Jpn. **46** (1979) 695.
 9. Ikeda T., Saeki Y. J. Phys. Soc. Jpn. **16** (1977) 1793.
 10. Martinez Sarrion M.L., Rodriques Clemente A., Mestres Vila L. J. Solid State Chem. **80** (1989) 235.
 11. Martinez Sarrion M.L., Rodriques Clemente A., Mestres Vila L. J. Solid State Chem. **84** (1990) 308.
 12. Sapriel J. Phys. Rev. (b) **12** (1975) 5128.
 13. Vlokh R., Vlokh O., Skab I., Romanyuk M. Ukr.J.Phys. **43** (1998) 80 (in Ukrainian).
 14. Vlokh R., Uesu Y., Yamada Y., Skab I., Vlokh O.V. J. Phys. Soc. Jpn (Letters) **67** (1998) 3335.
 15. Vlokh R.O., Vlokh O.V., Kabelka H., Warhanek H. Ferroelectrics **190** (1997) 89.
 16. Vlokh R., Kabelka H., Warhanek H., Skab I., Vlokh O.V. Phys. Stat. Sol.(a) **168** (1998) 397.
 17. Vlokh R., Skab I., Vlokh O., Uesu Y. Ukr.J.Phys.Opt. **2** (2001) 148.
 18. Vlokh R., Skab I., Vlokh O., Uesu Y., Yamada Y. Ferroelectrics **242** (2000) 47.
 19. Brezina B., Glogarova M. Phys. Stat. Sol. (a) **11** (1972) K39.
 20. Vlokh R., Skab I., Girnyk I., Czapla Z., Dacko S., Kosturek B. Ukr.J.Phys.Opt. **1** (2000) 28.
 21. Brezina B., Rivera J.-P., Schmid H. Ferroelectrics **55** (1984) 177.
 22. Vlokh R., Czapla Z., Kosturek B., Skab I., Vlokh O.V., Girnyk I. Ferroelectrics **219** (1998)
 23. Lissalde F., Abrahams S.C., Bernstein J.L., Nassau K. J. Appl. Phys. **50** (1979) 845.
 24. Bilecky I.N., Vlokh R.O., Otko A.I., Shopa Ya.I. Ukr.J.Phys. **33** (1988) 689 (in Russian).
 25. Adamiv V.T., Burak Y.V., Vasylechko L.O., Vlokh R.O., Girnyk I.S., Teslyuk I.M. Func. Mat. **5** (1998) 175.
 26. Vlokh R. Vlokh O., Kityk A., Skab I., Czapla Z., Kosturek B., Dacko S. Ferroelectrics **237** (2000) 481.
 27. Sannikov D.G Phys.Sol.State. **20** (1978) 837 (in Russian).
 - 27a. Antonenko A.M., Volnyanski M.D., Pozdeev V.G. Solid State Phys. **25** (1983) 1849 (in Russian).
 - 27b. Lissalde F., Abrahams S.C., Bernstein J.L. and Nassau K. J.Appl.Phys. **50** (1979) 845.
 - 27c. Hikita T., Sekiguchi H., Ikeda T. J.Phys.Soc.Japan **44** (1978) 243.
 - 27d. Maeda M., Ikeda T. J.Phys.Soc.Japan **47** (1979) 1581.
 28. Yamada N. J. Phys. Soc. Jpn. **46** (1979) 561.
 29. Glogarova M., Fousek J. Phys. Stat. Sol. (a) **15** (1973) 579.
 30. Vlokh R., Skab I., Girnyk I., Czapla Z., Dacko S., Kosturek B. Ukr. J. Phys. Opt. **1** (2000) 103
 31. Vlokh R., Skab I., Guzandrov A., Mogylyak I., Smaglyi S., Uesu Y. Ferroelectrics, **237** (2000) 489.